ELSEVIER

Catalysis Today 47 (1999) 295–303

CATALYSIS TODAY

# A study of Nusselt and Sherwood numbers in a monolith reactor

R.E. Hayes[a,*], S.T. Kolaczkowski[b]

[a]Department of Chemical and Materials Engineering, University of Alberta, Edmonton, Alta., CanadaT6G 2G6
[b]School of Chemical Engineering, University of Bath, Bath, BA2 7AY, UK

## Abstract

A two-dimensional model of a single channel of a monolith reactor is used to evaluate the values of the Nusselt and Sherwood numbers under reaction conditions. The circular channel is assumed to have axisymmetry with a first-order reaction occurring at the wall. The values of the Nusselt and Sherwood numbers do not correlate uniquely with the Graetz number but rather depend on the reaction rate at the wall. Hence they depend on such variables as gas velocity, inlet temperature and reactant concentration. © 1999 Elsevier Science B.V. All rights reserved.

*Keywords:* Catalytic combustion; Monolith reactor; Mass transfer

## 1. Introduction

The monolith honeycomb reactor is used in catalytic combustion applications, for example as an afterburning reactor in automobile exhaust systems. There is also interest in the development of gas turbines that use catalytic combustion to burn the fuel [1]. Another application is the selective catalytic reduction of $NO_x$ in effluent gases using ammonia [2].

Because of the importance of environmental issues, there have been hundreds of publications on catalytic combustion, covering materials, catalysts, reactor design, reaction kinetics and heat and mass transfer effects. This paper deals with aspects of heat and mass transfer in a circular channel of a honeycomb monolith reactor. Typical honeycomb reactors contain channels which are often of the order of 1–2 mm in diameter [3]. In auto exhaust applications the flow is in the laminar regime, while for gas turbine applications the flow may be either laminar or turbulent, depending on the operating conditions [1]. This study considers the laminar flow case. In a laminar flow tubular reactor, with gaseous reactants and an exothermic reaction, there is a radial velocity profile, with the velocity at the centreline being something less than twice the average velocity. The reactants are consumed by catalytic reaction at the wall with a concomitant release of thermal energy. Because of the laminar flow profile, there is the potential for radial concentration and temperature gradients. The magnitude of the radial gradients depends on the relative rates of mass and heat transfer and chemical reaction. In classical catalytic reactor analysis, the term kinetic control has been applied when the "bulk" fluid phase concentration and temperature are the same as those at the surface of the catalyst [4]. The rate of reaction is controlled by the intrinsic kinetics only. If the rate of

---

*Corresponding author.

PII: S0920-5861(98)00310-1

diffusion through the boundary layer is lower than the intrinsic rate of reaction, the bulk and surface conditions are different. In the extreme case the catalyst surface concentration approaches zero and the rate is controlled solely by the rate of mass transfer. This is known as mass transfer control. In a laminar flow reactor the concept is perhaps more nebulous because, after a certain entrance length has passed, the entire reactor is in essence a boundary layer. However, one can say that if the surface concentration were essentially zero then mass transfer is the dominant mechanism. The long held view on how monolith reactors operate was that at low temperatures the reaction was kinetically controlled. Typically this might occur in the reactor inlet region. At some point in the reactor, the rate of reaction would increase rapidly due to the Arrhenius temperature dependence of the rate constant(s); this point is sometimes referred to as light-off. The assumption is that after light-off the concentration at the wall approaches zero and the reaction is then mass transfer controlled. Many have held the view that light-off meant a change from kinetic to mass transfer control; i.e, at light-off the wall concentration suddenly dropped to essentially zero. It was recently demonstrated [5] that true mass transfer control may be difficult to achieve in a 1–2 mm diameter reactor channel at moderate temperatures, although it can be easily attained in larger diameter channels [6]. The wall concentration, however, is lower than the average radial concentration. Hayes and Kolaczkowski [5] defined a catalytic reaction number whose value determined whether or not a reaction was in the mass transfer or kinetic control regime.

The controversy over the controlling mechanism is not academic, and has led to some confusion in the literature concerning the values of the Sherwood and Nusselt numbers in a monolith reactor channel under reaction conditions. Correlations have been reported for Sherwood numbers [7,8] which gave values that were much lower than that expected, based on results from non-reacting systems, and lower than the values observed in reactor simulation studies [9]. The development of these correlations was based on experimental measurements and assumed a zero wall concentration. Hayes and Kolaczkowski [5] subsequently reanalysed these results using a two-dimensional model for the reactor and demonstrated that under their operating conditions the wall concentration was not zero, and hence the original analysis was faulty. They also concluded that after an initial inlet region the steady state Sherwood and Nusselt numbers had values of the same order of magnitude as those for the so-called Graetz problem, for constant property incompressible fluids flowing inside ducts with constant wall temperature or constant wall flux. These results were consistent with other modelling results [9–12]. These numerical results were reinforced by experiments [13].

The classical heat transfer problem of the flow of an incompressible Newtonian fluid in a duct with temperature independent physical properties is presented in most heat transfer textbooks [14]. In the fully developed region the Nusselt number achieves a constant value of 3.66 for a boundary condition of constant wall temperature and 4.364 for constant wall flux. The situation where the wall flux or temperature varies axially is discussed in [15]; the value of *Nu* often lies in between the two values quoted previously. In the developing region the value of *Nu* depends on whether or not the thermal boundary layer develops alone or in conjunction with a hydrodynamic boundary layer. The point is, however, that a unique solution is obtained in each case if the Nusselt number is plotted against the reciprocal Graetz number. Based on the heat and mass transfer analogy, similar results are found for the Sherwood number. For a monolith reactor, Hawthorn [16] proposed correlations for *Nu* and *Sh* numbers based on the earlier work of Kays and London [17] on laminar flow in ducts as follows:

$$Sh = 3.66\left\{1 + 0.095\frac{D_T}{L}Pe_{\mathrm{M}}\right\}^{0.45}, \tag{1}$$

$$Nu = 3.66\left\{1 + 0.095\frac{D_T}{L}Pe_{\mathrm{H}}\right\}^{0.45}. \tag{2}$$

These correlations have been used in the literature in the modelling of monolith reactors. One point to note is that these equations predict *average* values for the entire reactor length $L$. What is usually desired in a reactor model is a *local* value for the heat or mass transfer coefficient (i.e., the value as a function of $z$). The correlations (1) and (2) may lead to error if used to predict local values. This would be especially true where the entrance effects are important. Most modellers who use these correlations employ an average value over the entire monolith length [18,19]. Heck et al. [10] compared one- and two-dimensional models using the oxidation of CO as a representative reaction with LHHW type of kinetic model. Under certain inlet concentrations of CO, the Nusselt numbers exhibited sharp jumps at the point of light-off. This behaviour arises because of the form of the LHHW model; at some point the denominator term falls to 1 and the reaction rate suddenly increases by about an order of magnitude. This type of behaviour has not been observed with power law type kinetic models [5]. Heck et al. [10] stated that in the reactor entrance region up to the point of light-off, the *Nu* and *Sh* numbers corresponding to the condition of constant wall flux should be used. The light-off point gave rise to a new "entrance region" after the jump in *Nu*, for which the values corresponding to constant wall temperature should be used. They used the correlations for non-reacting fluids [20], i.e., for the constant wall temperature region:

$$Nu_{\mathrm{T}} = 3.655 + 6.874\left(\frac{Gz}{1000}\right)^{0.488} \exp\left(-\frac{57.2}{Gz}\right) \tag{3}$$

and

$$Nu_{\mathrm{H}} = 4.364 + 8.68\left(\frac{Gz}{1000}\right)^{0.506} \exp\left(-\frac{41.0}{Gz}\right) \tag{4}$$

for the constant wall flux region. Note that these two equations are for developing thermal flow with a fully developed velocity profile, not for a simultaneously developing thermal and hydrodynamic boundary layer. Hayes and Kolaczkowksi [5] also examined the Nusselt number behaviour using a two-dimensional model with LHHW kinetics. They observed the jump in *Nu* during transient operation, but observed that the effects of radiation and solid conduction combined to move the light-off point upstream to the entrance. Heck et al. [10] did not include the effects of conduction or radiation in their model. Similar results for the Sherwood number are obtained by substituting the Schmidt number, *Sc*, for the Prandtl number in the equation for the Graetz number.

Groppi et al. [21] proposed that a better solution for *Nu* in a system with chemical reaction at the wall was obtained by interpolating between $Nu_{\mathrm{T}}$ and $Nu_{\mathrm{H}}$ using the interpolation formula [22]:

$$\frac{Nu - Nu_{\mathrm{H}}}{Nu_{\mathrm{T}} - Nu_{\mathrm{H}}} = \frac{Da\,Nu}{(Da + Nu)Nu_{\mathrm{T}}}. \tag{5}$$

The Dämkohler number, *Da*, is the ratio of reaction rate to diffusion rate and depends on the reaction kinetics. For a first-order catalytic reaction expressed in terms of washcoat external surface area, i.e., $(-R_{\mathrm{A}})_S = k_S C_A$ where $k_S$ has units of m/s, the Dämkohler number is

$$Da = \frac{\eta k_S D_T}{4 D_{\mathrm{A}}}. \tag{6}$$

Note that the rate constant and diffusion coefficient were calculated at local conditions.

The fluid in a reactor is compressible with variable physical properties. Furthermore, the flux from the wall is not constant because of the diminution of the reactants and the increase in wall temperature that occurs as reactor length increases. It would therefore be surprising if the constant wall temperature or constant wall flux solutions matched with experimental results. It is also not obvious whether or not a single correlation should fit for all kinetics or operating conditions. Reliable values are certainly an asset if a heterogeneous one-dimensional model is used to simulate a laminar flow reactor, because heat and mass transfer coefficients are needed to couple the gas and solid phase conservation equations.

This paper reports a theoretical investigation of the Nusselt and Sherwood numbers in a single channel monolith reactor with emphasis on the entrance region. The effects of channel diameter, flow rate and temperature are considered. The objective was to determine the extent, if any, of the variation in the values of *Sh* and *Nu* with changing operating conditions, and to see if a single unique correlation would apply.

## 2. Formulation of the 2D model

The two-dimensional model was based on the solution of the axisymmetric momentum, mole and energy balance equations. Homogeneous reaction was ignored as it was considered likely to be insignificant in the temperature range studied. Heat loss radially through the walls was taken to be equal to zero. Radiation was also ignored.

A single monolith channel may be modelled in two dimensions by approximating the reactor as a right cylindrical tubular reactor of radius $R$ [9]. For axisymmetric steady state flow in a circular tube the radial and axial components of the equations of motion are [23]:

$$\rho\left(v_r\frac{\partial v_r}{\partial r}+v_z\frac{\partial v_r}{\partial z}\right)+\frac{\partial P}{\partial r}+\left(\frac{1}{r}\frac{\partial}{\partial r}(r\tau_{rr})+\frac{\partial \tau_{rz}}{\partial z}\right)=0, \tag{7}$$

$$\rho\left(v_r\frac{\partial v_z}{\partial r}+v_z\frac{\partial v_z}{\partial z}\right)+\frac{\partial P}{\partial z}+\left(\frac{1}{r}\frac{\partial}{\partial r}(r\tau_{rz})+\frac{\partial \tau_{zz}}{\partial z}\right)=0. \tag{8}$$

The equation of continuity in cylindrical coordinates is

$$\frac{1}{r}\frac{\partial}{\partial r}(\rho r v_r)+\frac{\partial}{\partial z}(\rho v_z)=0. \tag{9}$$

The components of the shear stress tensor for a Newtonian fluid are:

$$\tau_{rr}=-\mu\left[2\frac{\partial v_r}{\partial r}-\frac{2}{3}(\nabla\cdot v)\right], \tag{10}$$

$$\tau_{zz}=-\mu\left[2\frac{\partial v_z}{\partial z}-\frac{2}{3}(\nabla\cdot v)\right], \tag{11}$$

$$\tau_{rz}=-\mu\left[\frac{\partial v_z}{\partial r}+\frac{\partial v_r}{\partial z}\right]. \tag{12}$$

For an ideal gas with conservation of moles on reaction the $\nabla\cdot v$ term is given by

$$\nabla\cdot v=\frac{1}{T}\left(v_r\frac{\partial T}{\partial r}+v_z\frac{\partial T}{\partial z}\right)-\frac{1}{P}\left(v_r\frac{\partial P}{\partial r}+v_z\frac{\partial P}{\partial z}\right). \tag{13}$$

The boundary conditions used were flat or parabolic inlet velocity profile, zero slip condition at the walls, symmetry condition at the axis and zero normal shear stress at the outlet.

If the mole average velocity is assumed to be equal to the mass average velocity, then the steady state mole balance for component A is

$$\frac{1}{r}\frac{\partial}{\partial r}\left(rDC\frac{\partial Y_A}{\partial r}\right)+\frac{\partial}{\partial z}\left(DC\frac{\partial Y_A}{\partial z}\right)-C\left[v_r\frac{\partial Y_A}{\partial r}+v_z\frac{\partial Y_A}{\partial z}\right]=0. \tag{14}$$

The boundary conditions used were:

$$Y_A=Y_{A_0}\quad \text{at } z=0 \text{ and } r\neq R, \tag{15}$$

$$\frac{\partial Y_A}{\partial r}=0\quad \text{at } r=0 \text{ for all } z, \tag{16}$$

$$-DC\frac{\partial Y_A}{\partial r}=(-R_A)\quad \text{at } r=R \text{ for all } z, \tag{17}$$

$$\frac{\partial Y_A}{\partial z}=0\quad \text{at } z=L \text{ and } r\neq R. \tag{18}$$

The steady state energy balance equation for an ideal gas, ignoring viscous work terms, is

$$\frac{1}{r}\frac{\partial}{\partial r}\left(rk\frac{\partial T}{\partial r}\right)+\frac{\partial}{\partial z}\left(k\frac{\partial T}{\partial z}\right)-\rho C_P\left[v_r\frac{\partial T}{\partial r}+v_z\frac{\partial T}{\partial z}\right]=0. \tag{19}$$

The boundary conditions used were:

$$T=T_0\quad \text{at } z=0 \text{ and } r\neq R, \tag{20}$$

$$\frac{\partial T}{\partial z}=0\quad \text{at } z=L \text{ and } r\neq R, \tag{21}$$

$$\frac{\partial T}{\partial r}=0\quad \text{at } r=0 \text{ for all } z, \tag{22}$$

$$k\frac{\partial T}{\partial r}=(-\Delta H)(-R_A) \text{ at } r=R \text{ for all } z. \tag{23}$$

The $Nu$ and $Sh$ values can be computed from the radial temperature and concentration profiles obtained by the solution of the conservation of equations as follows:

$$Sh=\frac{2R}{(\langle Y_A\rangle-Y_{AW})}\frac{\partial Y}{\partial r}\bigg|_{r=R} \quad \text{and}$$

$$Nu=\frac{2R}{(T_W-\langle T\rangle)}\frac{\partial T}{\partial r}\bigg|_{r=R}, \tag{24}$$

where

$$\langle Y\rangle=\frac{\int_0^R v_z(r)Y_A(r)r\,\mathrm{d}r}{\int_0^R v_z(r)r\,\mathrm{d}r} \quad \text{and}$$

$$\langle T\rangle=\frac{\int_0^R v_z(r)\rho C_V T(r)r\,\mathrm{d}r}{\int_0^R v_z(r)\rho C_V r\,\mathrm{d}r}. \tag{25}$$

The solutions to the reactor model was generated using the Galerkin finite element method with triangular elements. Details of the method may be found in [6,9,24].

The combustion of methane in air was selected as a model reaction. This enabled realistic values of physical properties to be used. The rate expression was a first-order expression and, while not based explicitly on experimental data, gave values for the reaction rate of the same order as observed experimentally [1]. The rate expression used was

$$-R_{\mathrm{CH_4}} = 3 \times 10^5 \exp\left(-\frac{100000}{R_g T}\right) C_A, \qquad (26)$$

where the rate has units of mol/m$^2$ s and the activation energy is in J/mol. Although diffusion limitation in the washcoat would be expected to become important at temperatures greater than about 750 K [13], this was ignored in this investigation. The diffusion coefficient for methane in air was calculated from the Fuller correlation [25]:

$$D = 9.99 \times 10^{-5} \frac{T^{1.75}}{P} \qquad (27)$$

with $T$ in K, $P$ in Pa and $D$ in m$^2$/s. The thermal conductivity of the fluid was calculated by

$$k = 1.679 \times 10^{-2} + 5.073 \times 10^{-5} T, \qquad (28)$$

where $k$ has the units of W/m s. The viscosity of the fluid in Pa s was computed from

$$\mu = 7.701 \times 10^{-6} + 4.166 \times 10^{-8} T - 7.531 \times 10^{-12} T^2. \qquad (29)$$

## 3. Nusselt and Sherwood numbers

In this section the results obtained from the two-dimensional simulator are presented. The effects of inlet gas temperature, inlet mole fraction of methane in the feed and inlet velocity were examined. A summary of the simulations is presented in Table 1. The Nusselt numbers were plotted as a function of the inverse Graetz number with the results presented in Figs. 1–5. The following observations can be made about the results.

The Nusselt number predicted in the simulations is of the same order of magnitude as that predicted for the situation of constant wall temperature and constant wall flux. This confirms other simulations reported in the literature, and is as expected.

The Nusselt number predicted in the simulations did not match the Nusselt numbers calculated using the boundary conditions of constant wall temperature and constant wall flux. As noted previously, because neither of these two boundary conditions represents the actual boundary condition, this is not too surprising.

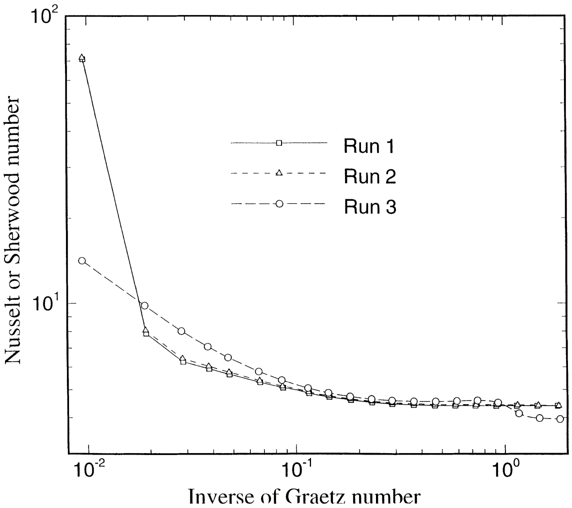

Fig. 1. Effect of inlet concentration on the Nusselt and Sherwood number. All runs at gas inlet temperature of 700 K and velocity 1 m/s. Inlet mole fractions: Run 1 – 0.001; Run 2 – 0.005; Run 3 – 0.01. Refer to Table 1 for complete details of operating conditions.

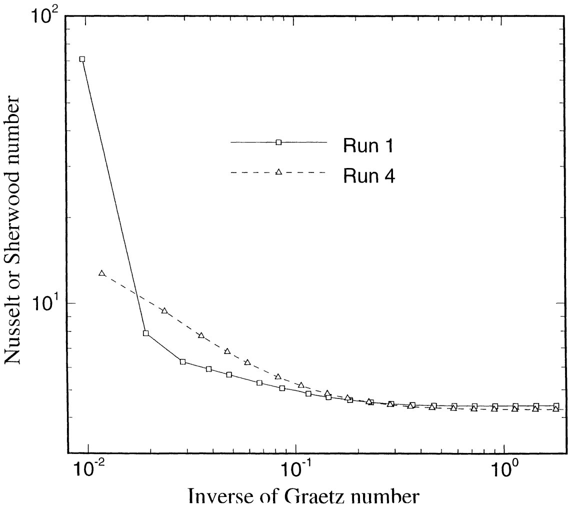

Fig. 2. Effect of inlet gas temperature on Nusselt and Sherwood number. Both runs at inlet mole fraction of 0.001 and velocity 1 m/s. Inlet gas temperatures: Run 1 – 700 K; Run 4 – 800 K. Refer to Table 1 for complete details of operating conditions.

Table 1
Summary of conditions used in the simulations (outlet values are based on a 20 mm long reactor)

| Experiment | Inlet mole fraction of methane | Inlet gas temperature (K) | Inlet velocity (m/s) | Combined entry length | | | Thermal concentration entry lengths only | | |
|---|---|---|---|---|---|---|---|---|---|
| | | | | Outlet $X$ (%) | Outlet gas temperature (K) | $Nu_{\mathrm{FD}}$ | Outlet $X$ (%) | Outlet gas temperature (K) | $Nu_{\mathrm{FD}}$ |
| 1 | 0.001 | 700 | 1 | 32.9 | 709 | 4.39 | 31.7 | 708 | 4.39 |
| 2 | 0.005 | 700 | 1 | 57.4 | 774 | 4.40 | 53.7 | 768 | 4.40 |
| 3 | 0.01 | 700 | 1 | 99.6 | 948 | 3.96 | 99.4 | 947 | 3.96 |
| 4 | 0.001 | 800 | 1 | 95.1 | 824 | 4.26 | 94.5 | 824 | 4.26 |
| 5 | 0.005 | 800 | 1 | 100 | 925 | 4.01 | 99.9 | 925 | 4.01 |
| 6 | 0.01 | 800 | 1 | 100 | 1045 | 3.77 | 100 | 1045 | 3.77 |
| 7 | 0.001 | 700 | 3 | 11.7 | 702 | 4.40 | 11.3 | 702 | 4.40 |
| 8 | 0.005 | 700 | 3 | 14.5 | 718 | 4.43 | 13.8 | 717 | 4.43 |
| 9 | 0.01 | 700 | 3 | 23.2 | 758 | 4.56 | 21.7 | 755 | 4.56 |
| 10 | 0.001 | 700 | 2 | 17.4 | 705 | 4.40 | 16.6 | 704 | 4.40 |
| 11 | 0.005 | 700 | 2 | 23.5 | 730 | 4.43 | 22.2 | 728 | 4.43 |
| 12 | 0.01 | 700 | 2 | 59.7 | 850 | 4.54 | 53.8 | 835 | 4.54 |
| 13 | 0.001 | 700 | 6 | 5.9 | 701 | 4.44 | 5.7 | 701 | 4.44 |
| 14 | 0.005 | 700 | 6 | 6.7 | 708 | 4.48 | 6.5 | 708 | 4.48 |
| 15 | 0.01 | 700 | 6 | 8.2 | 720 | 4.54 | 8.0 | 720 | 4.54 |

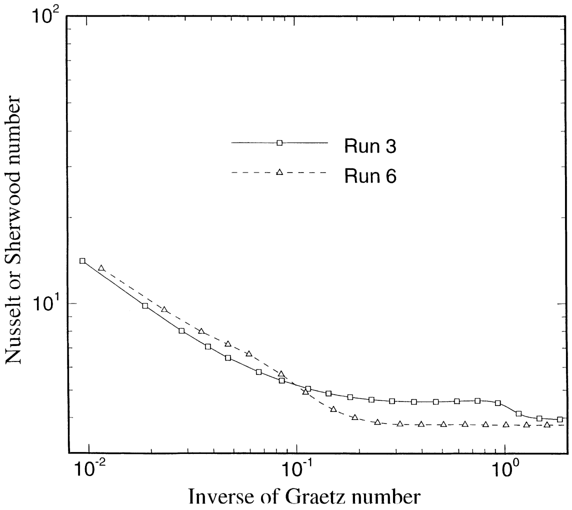

Fig. 3. Effect of inlet gas temperature on Nusselt and Sherwood number. Both runs at inlet mole fraction of 0.01 and velocity 1 m/s. Inlet gas temperatures: Run 3 – 700 K; Run 6 – 800 K. Refer to Table 1 for complete details of operating conditions.

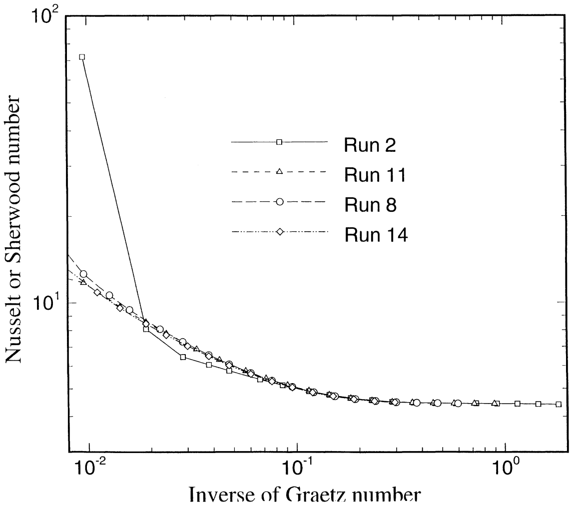

Fig. 4. Effect of inlet gas velocity on Nusselt and Sherwood number. All runs at inlet mole fraction of 0.005 and inlet gas temperature 700 K. Inlet velocities: Run 2 – 1 m/s; Run 11 – 2 m/s; Run 8 – 3 m/s; Run 14 – 6 m/s. Refer to Table 1 for complete details of operating conditions.

If we consider the interpolation formula of Eq. (5), one observation may be made. The value of $Da$ for any given rate expression is a function only of temperature and pressure. The pressure was held constant in all runs, therefore at a gas inlet temperature of 700 K the

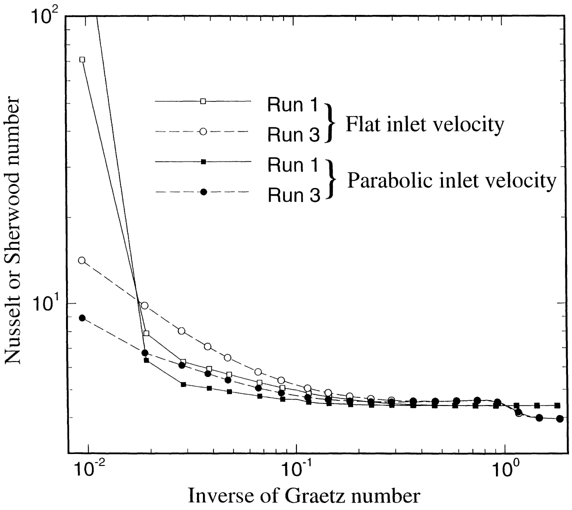

Fig. 5. Effect of inlet gas velocity profile on Nusselt and Sherwood number. All runs at inlet gas temperature of 700 K and mean inlet velocity 1 m/s. Inlet mole fractions: Run 1 – 0.001; Run 3 – 0.01. Refer to Table 1 for complete details of operating conditions.

value of the fully developed Nusselt number should be a constant 4.30 regardless of the value of inlet velocity and concentration. From Table 1 it can be seen that this is not the case, and numbers in the range 3.77–4.56 are seen. Following the same logic, for constant inlet temperature, the plot of $Nu$ vs. $Gz^{-1}$ should also be coincident if the inlet temperature is the same. In fact, examining Figs. 1–5 considerable variation is seen.

There is a difference observed when the fluid enters the reactor with a fully developed profile compared to when it enters with a flat profile. Because the Prandtl number of the fluid is approximately 0.7, the hydrodynamic and thermal boundary layer develops at about the same rate, so a difference between the two cases is expected. It should be pointed out that Eqs. (3) and (4) were developed for the case of a developing thermal boundary layer with hydrodynamically fully developed flow. In a monolith reactor, the usual situation would be simultaneously developing flow, temperature and concentration profiles.

It is evident that the prediction of heat and mass transfer coefficients in the circular monolith channel is not straightforward. The situation is likely to be more complex in cases where the reaction is not a simply first-order reaction or where multiple reactions occur. In cases where there can be sudden changes in reaction rate (such as with LHHW type kinetics) the situation is quite complex indeed [5]. In non-circular channels where the reaction rate (and hence heat flux) may vary around the perimeter, the situation will be more complicated.

## 4. Conclusions

This paper has examined the Nusselt and Sherwood numbers in a monolith reactor channel with first-order reaction at the wall. The following conclusions were drawn:

1. The Nusselt and Sherwood numbers for the case in which chemical reaction occurs at the wall are not the same as those observed in either the constant wall temperature or the constant wall flux cases.
2. A simple interpolation between the value for constant wall temperature and constant wall flux using the Dämkohler number calculated at inlet reactor conditions does not predict exactly the observed value of Nusselt number.
3. When calculating the value of Nusselt and Sherwood numbers, it is important to include the effects of simultaneous development of thermal, concentration and hydrodynamic boundary layers.
4. In monolith channels of other cross-sectional shapes, where axisymmetry does not exist the situation is likely to be more complex, because of the possibility of variable reaction rate around the perimeter of the channel.

## 5. Nomenclature

| | |
|---|---|
| $C$ | molar density of the gas (mol/m$^3$) |
| $C_{\mathrm{A}}$ | concentration of species A (mol/m$^3$) |
| $C_P$ | constant pressure heat capacity (J/mol K) |
| $C_V$ | constant volume heat capacity (J/mol K) |
| $Da$ | Dämkohler number |
| $D$ | molecular diffusion coefficient (m$^2$/s) |
| $D_T$ | channel diameter (m) |
| $Gz$ | Graetz number |
| $k$ | thermal conductivity of the gas (W/m s) |
| $k_S$ | reaction rate constant expressed in terms of washcoat surface area |
| $L$ | length of the reactor (m) |
| $Nu$ | Nusselt number; mean bulk conditions |
| $Nu_{\mathrm{H}}$ | Nusselt number, constant surface heat flux boundary condition |
| $Nu_{\mathrm{T}}$ | Nusselt number, constant wall temperature boundary condition |
| $P$ | pressure of the gas (Pa) |
| $Pe_{\mathrm{M}}$ | Peclet number for mass transfer |
| $Pe_{\mathrm{H}}$ | Peclet number for heat transfer |
| $r$ | radial coordinate (m) |
| $R$ | radius of the monolith channel (m) |
| $-R_{\mathrm{A}}$ | catalytic reaction rate of component A, rate of disappearance (mol/m$^2$ s) |
| $R_{\mathrm{g}}$ | gas constant (J/mol K) |
| $Sc$ | Schmidt number |
| $Sh$ | Sherwood number |
| $T$ | temperature (K) |
| $\langle T\rangle$ | average gas temperature (K) |
| $T_{\mathrm{W}}$ | temperature of the wall (K) |
| $v$ | velocity (m/s) |
| $v_r$ | radial velocity (m/s) |
| $v_z$ | axial velocity (m/s) |
| $Y_{\mathrm{A}}$ | mole fraction of component A |
| $\langle Y_{\mathrm{A}}\rangle$ | average mole fraction of component A across a cross-section |
| $Y_{\mathrm{AW}}$ | mole fraction of A at the wall |
| $z$ | axial coordinate (m) |

*Greek letters*

| | |
|---|---|
| $\mu$ | viscosity of the gas (Pa s) |
| $\rho$ | mass density of the gas (kg/m$^3$) |
| $\tau$ | stress tensor |
| $\Delta H$ | enthalpy change on reaction (J/mol) |

## Acknowledgements

The authors acknowledge financial support from NSERC (Canada) and EPSRC (UK).

## References

[1] S.T. Kolaczkowski, Trans. I. Chem. E, Part A 73 (1995) 168; Errata 73 (1995) 865.
[2] S.M. Cho, Chem. Eng. Prog. 90(1) (1994) 39.
[3] W.J. Thomas, Chemistry and Industry (1986) 315.
[4] C.N. Satterfield, Mass Transfer in Heterogeneous Catalysis, MIT Press, Cambridge, MA.
[5] R.E. Hayes, S.T. Kolaczkowski, Chem. Eng. Sci. 49(21) (1994) 3587.

[6] A.J. Rankin, R.E. Hayes, S.T. Kolaczkowski, Trans. I. Chem. E, Part A 73 (1995) 110.

[7] C.J. Bennett, S.T. Kolaczkowski, W.J. Thomas, Trans. I. Chem. E, Part B 69 (1991) 209.

[8] U. Ullah, S.P. Waldrum, C.J. Bennett, T. Truex, Chem. Eng. Sci. 47(9)(10)(11) (1992) 2413.

[9] R.E. Hayes, S.T. Kolaczkowski, W.J. Thomas, Computers Chem. Eng. 16(7) (1992) 645.

[10] R.H. Heck, J. Wei, J.R. Katzer, AIChE J. 22(3) (1976) 477.

[11] L.C. Young, B.A. Finlayson, AIChE J. 22(2) (1976) 343.

[12] S. Lee, R. Aris, Chem. Eng. Sci. 32 (1977) 827.

[13] S.T. Kolaczkowski, W.J. Thomas, J. Titiloye, D.J. Worth, Combustion Sci. Tech. 118 (1996) 79–100.

[14] F.P. Incropera, D.P. DeWitt, Introduction to Heat Transfer, Wiley, New York, 1990.

[15] W.M. Kays, M.E. Crawford, Convective Heat and Mass Transfer, 3rd ed., McGraw-Hill, New York, 1993.

[16] R.D. Hawthorn, AIChE Symp. Ser. 70(137) (1974) 428.

[17] W.M. Kays, A.L. London, Compact Heat Exchangers, 2nd ed., McGraw-Hill, New York, 1964.

[18] T. Ahn, W.V. Pinczewski, D.L. Trimm, Chem. Eng. Sci. 41 (1986) 55.

[19] J.W. Beekman, L.L. Hegedus, Ind. Eng. Chem. Res. 30(5) (1991) 969.

[20] V. Grigull, H. Tratz, Int. J. of Heat Mass Trans. 8 (1995) 669.

[21] G. Groppi, A. Betolli, E. Tronconi, P. Forzatti, Chem. Eng. Sci. 50 (1995) 2705.

[22] H.W. Brauer, F. Fetting, Chem. Eng. Technol. 38 (1966) 30.

[23] R.B. Bird, W.E. Stewart, E.N. Lightfoot, Transport Phenomena, Wiley, Toronto, 1960.

[24] A.J. Rankin, Polychlorinated biphenyl combustion in a monolith reactor, M.Sc. Thesis, University of Alberta, 1993.

[25] E.N. Fuller, P.D. Schettler, J.C. Giddings, Ind. Eng. Chem. 58 (1966) 19.